Protocol for Generating Optical Gottesman-Kitaev-Preskill States with Cavity QED

Hastrup, Jacob; Andersen, Ulrik L.

Published in:
Physical Review Letters

Link to article, DOI:
10.1103/PhysRevLett.128.170503

Publication date:
2022

Document Version
Publisher's PDF, also known as Version of record

Protocol for Generating Optical Gottesman-Kitaev-Preskill States with Cavity QED

Jacob Hastrup* and Ulrik L. Andersen
Center for Macroscopic Quantum States (bigQ), Department of Physics, Technical University of Denmark, Building 307, Fysikvej, 2800 Kongens Lyngby, Denmark

(Received 10 May 2021; accepted 22 February 2022; published 27 April 2022)

Gottesman-Kitaev-Preskill (GKP) states are a central resource for fault-tolerant optical continuous-variable quantum computing. However, their realization in the optical domain remains to be demonstrated. Here we propose a method for preparing GKP states using a cavity QED system that can be realized in several platforms, such as trapped atoms, quantum dots, or diamond color centers. We then further combine the protocol with the previously proposed breeding protocol by Vasconcelos *et al.* to relax the demands on the quality of the QED system, finding that GKP states with more than 10 dB squeezing could be achieved in near-future experiments.

DOI: 10.1103/PhysRevLett.128.170503

Introduction.—Quantum error correction is an essential step toward building large-scale quantum computers with realistic noisy components. In 2001, Gottesman, Kitaev, and Preskill (GKP) proposed an error correction protocol in which each qubit is encoded into the continuous variables of an infinite-dimensional bosonic mode [1]. With this encoding, small amounts of losses or small displacements errors [2,3] can be corrected using only Gaussian operations, provided a supply of high-quality GKP-encoded states. GKP error correction is particularly suitable in combination with optical cluster states [4–7], a field which has seen tremendous progress in recent years [8–10]. Additionally, GKP error correction can be used in long distance quantum communication schemes [11,12], implementing quantum repeaters using only beam splitters, homodyne detectors, and GKP ancilla resource states [13].

However, the required GKP states are non-Gaussian and have proven extremely difficult to produce experimentally. A central complexity for GKP-based error correction is thus the question on how to generate the GKP states themselves. Only in recent years have the states been produced in the motional mode of a trapped ion [14,15] and in a microwave cavity field coupled to a superconducting circuit [16]. Yet, the techniques relevant for generating stationary GKP states [17,18] in those experiments are not readily applicable for generating flying GKP states in an optical regime. Crucially, GKP states therefore remain to be demonstrated in the optical domain, despite several proposed generation schemes [19–24]. One promising approach is to interfere squeezed states on a multimode interferometer and project one output mode into an approximate GKP state by measuring the remaining modes with photon number resolving detectors [5,23]. Progress in high-quality photon number resolving detectors could make this experiment feasible in the near future. However, the method is fundamentally probabilistic and thus needs multiplexing to be scalable, which imposes a large resource overhead. Furthermore, it is unclear how efficient and noise tolerant the protocol is for generating highly squeezed GKP states (> 10 dB squeezing), which are likely required to achieve fault tolerance [6,7,25].

Another proposal is to build the GKP state using squeezed Schrödinger's cat states as the non-Gaussian element [21,22]. The advantage of this approach is that it uses only beam splitters and homodyne detectors, and that it can be made fully deterministic [22]. However, it requires large amplitude cat states, which are challenging to produce in optics. Still, recently Hacker *et al.* demonstrated the experimental generation of optical cat states by reflecting a light pulse off an optical cavity containing an atom [26]. This method can, in principle, be used to generate cat states of arbitrary amplitude, although the method requires both high cooperativity and large escape efficiency, which is experimentally challenging.

In this work, inspired by the experimental progress reported in [26], we propose to use cavity quantum electrodynamics (QED) to generate optical flying approximate GKP states by iteratively reflecting squeezed states off a cavity containing a three-level system. We thus extend the cat state generation protocol of [26] by inputting squeezed states and by applying multiple interactions. We analyze the performance in systems with finite cooperativity and nonunity escape efficiency to determine the expected quality of the produced state with realistic devices. We then combine the protocol with the cat state breeding protocol of Ref. [21], which turns out to heavily relax the requirements on the quality of the cavity QED system. We also derive analytical expressions for the optimal cavity QED parameters which minimize excess losses and provide a stable interaction across a broader frequency bandwidth, thus enabling the protocol to be used with temporally fast optical pulses. Finally, we propose a method to generate the

input squeezed states also using the cavity QED system, eliminating the need for a squeezed light source at the cavity QED resonance frequency.

Preliminaries.—GKP states: We describe the optical mode as a single bosonic mode with annihilation and creation operators $\hat{a}$ and $\hat{a}^\dagger$ and corresponding quadrature operators $\hat{x} = (1/\sqrt{2})(\hat{a} + \hat{a}^\dagger)$ and $\hat{p} = (1/\sqrt{2}i)(\hat{a} - \hat{a}^\dagger)$ satisfying $[\hat{x}, \hat{p}] = i$. The aim of our work is to produce good approximate GKP states with a square lattice. In this Letter, the relevant approximation is a finite superposition of squeezed states [27],

$$|0_{\mathrm{GKP}}\rangle \propto \sum_s \hat{D}\,(\sqrt{2\pi}s)\hat{S}(r)|\mathrm{vac}\rangle,$$
$$|1_{\mathrm{GKP}}\rangle \propto \hat{D}(\sqrt{\pi/2})|0_{\mathrm{GKP}}\rangle, \tag{1}$$

where $\hat{D}(\alpha) = \exp(\alpha\hat{a}^\dagger - \alpha^*\hat{a})$ is the displacement operator and $\hat{S}(r) = \exp\left(\frac{1}{2}(r^*\hat{a}^2 - r\hat{a}^{\dagger 2})\right)$ is the squeezing operator. The summation index s is over a finite number of integers around zero. GKP states have a periodic comb structure in both x and p quadratures with high-quality GKP states consisting of highly squeezed peaks in both quadratures. Large squeezing in x is achieved with large r as is evident from Eq. (1), while large squeezing in p is achieved by including many terms in the sum. For a finite number of terms, the squeezing in p can be further improved by weighing the superposition of Eq. (1) such that terms further from the origin have less weight. In this Letter, we quantify the quality of the produced GKP states by their amount of effective squeezing [28] in each quadrature, defined as

$$\Delta_x = \sqrt{\frac{1}{2\pi}\ln\left(\frac{1}{|\langle\hat{D}(i\sqrt{2\pi})\rangle|^2}\right)}, \tag{2}$$

$$\Delta_p = \sqrt{\frac{1}{2\pi}\ln\left(\frac{1}{|\langle\hat{D}(\sqrt{2\pi})\rangle|^2}\right)}. \tag{3}$$

The amount of squeezing is commonly denoted in decibels as $\Delta_{\mathrm{dB}} = -10\log_{10}(\Delta^2)$. For the approximate GKP state of Eq. (1) one obtains $\Delta_x = e^{-r}$, while Δ_p depends on the number of terms, e.g., $\Delta_p = (6.6, 10.4, 13.7)$ dB for (2,4,8) terms, respectively [18].

Cavity QED system: Since GKP states are non-Gaussian, we require a non-Gaussian element to generate them. In this Letter, we propose to use a cavity QED system as the central and only non-Gaussian element. In particular, we consider the reflection of an incoming optical field onto a single-mode cavity containing a three-level system, as depicted in Fig. 1(a). The three-level system consists of two low-energy states $|0\rangle$ and $|1\rangle$ and one high-energy state $|e\rangle$, which can be optically excited from the state $|1\rangle$ through a Jaynes-Cummings Hamiltonian with coupling strength g.

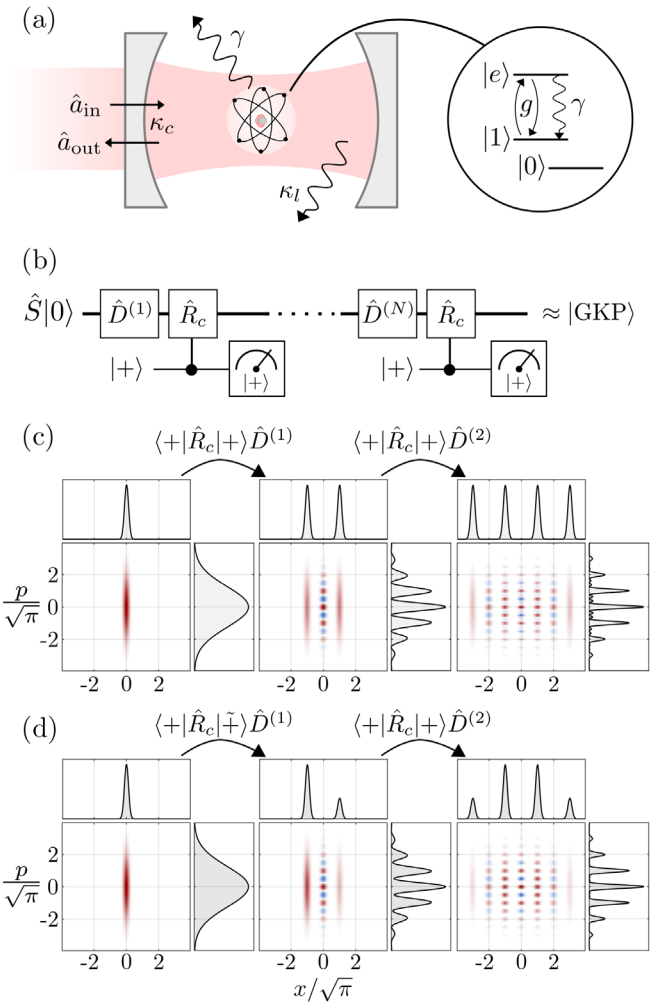

FIG. 1. (a): Cavity QED system consisting of a cavity containing a three-level system in which two levels resonantly couple to the cavity field. The cavity couples to a free-space field with rate κ_c and to undesired scattering and loss modes with rate κ_l. Additionally, the excited state of the three-level system can spontaneously decay through modes different from the cavity mode with rate γ. Ideally, the cavity imprints a controlled rotation $\hat{R}_c$ [Eq. (4)], on the reflection of an incoming mode. (b) Circuit diagram for the GKP state generation protocol. (c) Repeated applications of displacements and controlled rotations evolves an initial squeezed vacuum state into an approximate GKP state. The figure shows simulations of the Wigner function and quadrature distributions of an input state undergoing ideal interactions. (d) Preparing the atom in an unequal superposition $|\tilde{+}\rangle$ in the second to last step allows for the final state to have a two-level amplitude weighting of the squeezed peaks.

In this Letter, we denote this three-level system as an "atom," e.g., as the one used in the experiment of [26]. However, this atom could also be artificial such as a charged quantum dot [29–31] with the states $|0\rangle$ and $|1\rangle$ denoting spin states and $|e\rangle$ denoting a charged exciton state, or it could be a diamond color center [32,33], such as the nitrogen- or silicon-vacancy centers, where the states

$|0\rangle$ and $|1\rangle$ are represented by spin ground states and $|e\rangle$ is an excited spin state. The cavity resonance frequency and the frequency of the incoming field are equal and tuned to match the $|1\rangle \leftrightarrow |e\rangle$ transition. To couple light into and out of the cavity, one end of the cavity is constructed with a slightly transparent mirror with a coupling rate κ_c to an external free-space field. With the atom prepared in the $(|0\rangle, |1\rangle)$ subspace, an optical field mode reflected on the cavity ideally experiences a controlled phase rotation $\hat{R}_c$, depending on the state of the atom [26,34],

$$\hat{R}_c \equiv e^{i\pi\hat{n}} \otimes |0\rangle\langle 0| + \hat{\mathbb{I}} \otimes |1\rangle\langle 1|. \tag{4}$$

If the atom is initially in the state $|+\rangle = (|0\rangle + |1\rangle)/\sqrt{2}$, an incoming optical state $|\psi\rangle$ evolves as

$$\hat{R}_c|\psi\rangle \otimes |+\rangle = (e^{i\pi\hat{n}}|\psi\rangle \otimes |0\rangle + |\psi\rangle \otimes |1\rangle)/\sqrt{2}. \tag{5}$$

Subsequently, measuring the atom in state $|+\rangle$ yields

$$\langle +|\hat{R}_c|\psi\rangle \otimes |+\rangle = (e^{i\pi\hat{n}}|\psi\rangle + |\psi\rangle)/\sqrt{2}. \tag{6}$$

For example, for a coherent state input we obtain a Shrödinger's cat state, as was recently experimentally demonstrated [26].

Realistic systems, however, are limited by losses and scattering into unwanted modes at rate κ_l, as well as spontaneous decay of the excited state of the atom through modes different than the cavity mode at rate γ. In the Supplemental Material [35], we describe how to model these imperfections. The imperfections are conveniently described by the cooperativity

$$C = \frac{g^2}{2\gamma\kappa} \tag{7}$$

and escape efficiency

$$\eta = \frac{\kappa_c}{\kappa}, \tag{8}$$

where $\kappa = \kappa_l + \kappa_c$ is the total cavity loss. Both C and η should preferably be as large as possible. However, there is a trade-off between the cooperativity and the escape efficiency. This is because the cooperativity can be increased by decreasing κ_c, while the escape efficiency is increased by increasing κ_c. Since we would like both high cooperativity and high escape efficiency, one has to carefully tune the cavity coupling rate by engineering the cavity design. In the following, we therefore quantify the system in terms of the internal cooperativity [39], defined as

$$C_0 = \frac{g^2}{2\kappa_l\gamma} = \frac{C}{1-\eta}. \tag{9}$$

Thus, for fixed g, κ_l, and γ, the internal cooperativity does not depend on the coupling rate κ_c. Note also that the internal cooperativity is always larger than the actual cooperativity, $C_0 \geq C$. In the Supplemental Material [35], we analytically estimate the optimal value of κ_c to be

$$\kappa_c^{\text{opt}} = \sqrt{\frac{\kappa_l}{\gamma}(g^2 + \gamma\kappa_l)}. \tag{10}$$

In the following analysis, we numerically optimize κ_c for each C_0 in order to optimize the effective squeezing of the output states.

Results.—The idea of our proposed protocol is to repeatedly use the controlled rotation imposed by the cavity to generate an approximate GKP state, as illustrated in Figs. 1(b) and 1(c). That is, inputting a displaced squeezed vacuum state, we obtain a squeezed Schrödinger's cat state. Displacing and reflecting the output state on the cavity again further doubles the number of squeezed peaks in the output state and repeating this N times yields a state of the form of Eq. (1) with 2^N peaks. The displacement amplitude at the at nth step is given by

$$\hat{D}_n = \hat{D}(2^{n-1}\sqrt{\pi/2}). \tag{11}$$

For a sufficiently squeezed input state, the probability to obtain the measurement result $|+\rangle$ N times is $1/2^N$. However, the first interaction can be made deterministic, by adding a feed-forward displacement operation since

$$\begin{aligned}&\hat{D}(i\sqrt{\pi}/(2\sqrt{2}))(\hat{D}(\sqrt{2\pi}) - \hat{D}(-\sqrt{2\pi}))\hat{S}(r)|\text{vac}\rangle \\ &\quad \approx (\hat{D}(\sqrt{2\pi}) + \hat{D}(-\sqrt{2\pi}))\hat{S}(r)|\text{vac}\rangle.\end{aligned} \tag{12}$$

Thus a four peak state, which can yield up to 10.4 dB squeezing, can be generated with probability 0.5, while an eight peak state, yielding up to 13.7 dB squeezing, can be generated with probability 0.25.

The solid lines of Fig. 2(a) show the obtainable amount of squeezing using the protocol with finite-cooperativity systems. In addition to optimizing κ_c, we also numerically optimize the amount of input squeezing (see Supplemental Material [35] for details on the input squeezing). The optimization is done by optimizing $\min(\Delta_x, \Delta_p)$ (in units of decibels) such that we ensure effective squeezing in both quadratures. Additionally, we can slightly further improve the performance by slightly tuning the displacement amplitudes and the atomic superposition state (details in the Supplemental Material [35]).

The dashed lines of Fig. 2(a) show the result when implementing these two modifications. Note that, for both the solid and dashed lines, there exists an optimal number of interactions N for each value of the internal cooperativity. This is because the effects of noise due to γ and κ_l add up over multiple interactions. Additionally, as more interactions are applied, the photon number of the state

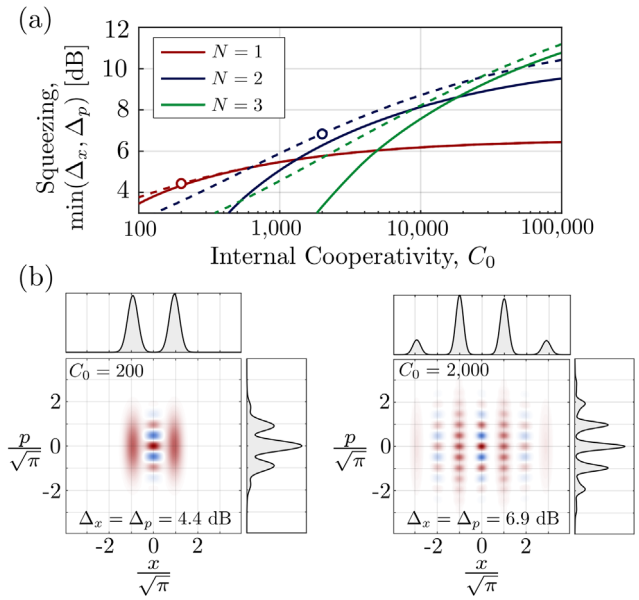

FIG. 2. (a) Achievable amount of effective squeezing generated by the protocol outlined in Fig. 1 using a cavity with finite cooperativity and nonunity escape efficiency, as a function of internal cooperativity C_0 [Eq. (9)], optimizing the cavity output coupling rate and the input squeezing parameter. N denotes the number of interactions with the cavity. The dashed lines further optimize over the displacement magnitudes and the initial state of the atom. (b) Wigner functions and quadrature distributions for the states generated with $C_0 = 200$ and $C_0 = 2000$ using $N = 1$ and $N = 2$, respectively, corresponding to open circles in (a).

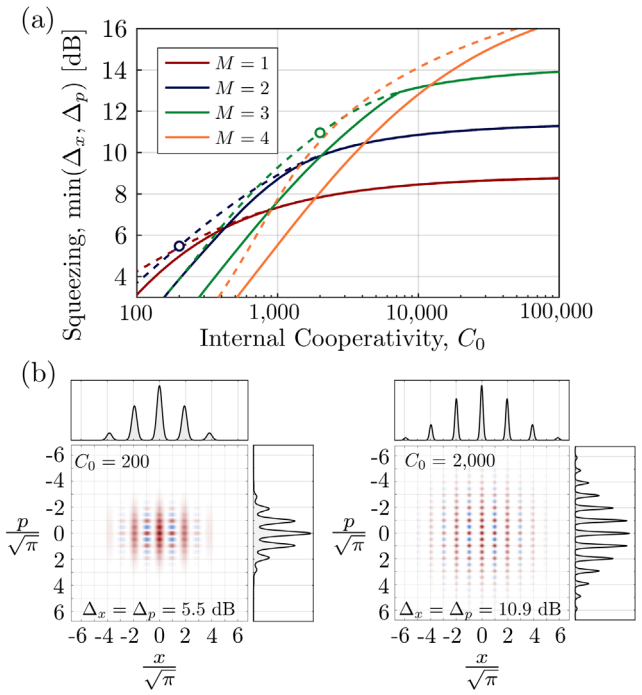

FIG. 3. Achievable amount of effective squeezing obtained with the cat state breeding method [21], using input squeezed cat states generated with the cavity QED system. M refers to the number of rounds of the breeding protocol. The dashed lines show the result when fine-tuning the displacement amplitude to partly compensate losses in the cavity. (b) Wigner functions and quadrature distributions using $C_0 = 200$ and $C_0 = 2000$ with $M = 2$ and $M = 3$, respectively, corresponding to the points marked with open circles in (a).

increases, making the state more vulnerable to loss from subsequent interactions. Thus, at some point, the noise added outweighs the effect of increasing the number of peaks in the state. Figure 2(b) shows the Wigner functions and quadrature probability distributions of the achievable states with $C_0 = 200$ and $N = 1$ (left) and $C_0 = 2000$ and $N = 2$ (right). For $C_0 = 200$ the produced state is essentially a squeezed Schrödinger's cat state, but the quadrature distributions reveal the onset of the desired comblike structure. For $C_0 = 2000$ we see a clear grid structure in the Wigner function and a narrowing of the peaks in the quadrature distribution.

As is evident from Fig. 2, the protocol demands very high values of the internal cooperativity to produce high-squeezing grid states. This is due to the multiple interactions required with the noisy cavity, as well as the demanding simultaneous requirements of high cooperativity and high escape efficiency.

To reduce the demands on the cavity QED system, we propose to combine the protocol with the Schrödinger's cat-state-based breeding protocol of Ref. [21]. In that protocol, we begin with a squeezed cat state of the form

$$|\mathrm{sqcat}\rangle = [\hat{D}(\sqrt{\pi}\sqrt{2}^{M-1}) + \hat{D}(-\sqrt{\pi}\sqrt{2}^{M-1})]\hat{S}(r)|\mathrm{vac}\rangle, \tag{13}$$

where M is the number of iterations of the breeding protocol. Two such squeezed cat states are combined on a 50:50 beam splitter and the p quadrature of one mode is measured with a homodyne detector. Conditioned on the result $p = 0$, the other mode is projected into an approximate GKP-like state. This protocol is then iterated, combining two such output states on another 50:50 beam splitter and projecting one mode out with homodyne detection, etc. After M iterations, the resulting output is an approximate GKP state of which Δ_p decreases with the number of iterations and Δ_x equals the squeezing of the initial input cat states. One important feature of this breeding protocol is that homodyne detectors and beam splitters can be implemented with near-unity efficiency. Thus, the experimental challenges are focused on producing high-quality squeezed cat states. Note from Eq. (13) that the amplitude of the initial squeezed cat states depends on the number of iterations M. Thus, to achieve a highly squeezed approximate GKP state, we require a large amplitude squeezed cat state, which is more sensitive to noise, such as loss, and thus experimentally more demanding.

A deterministic version of this protocol was proposed in [22], by adding a feed-forward displacement to the final

state. Furthermore, it was shown in [22] that this deterministic approach on average generated GKP states with ∼1 dB more squeezing compared to the probabilistic approach.

Figure 3(a) shows the obtainable amount of effective squeezing generated with the breeding protocol, using squeezed cat states produced by a single reflection on the cavity. As with Fig. 2, we also optimize the displacement of the squeezed cat state, with the results shown by the dashed lines. We see a substantial increase in the amount of achievable squeezing, reaching more than 10 dB for an internal cooperativity around $C_0 = 1300$, corresponding to a cooperativity of $C = 25$ and escape efficiency $\eta = 0.98$. Note that we have to generate 2^M squeezed cat states to breed each approximate GKP state. Even though each of these squeezed cat states are generated under noisy conditions, they still breed into an approximate GKP state with more squeezing than what is possible solely using the cavity. Figure 3(b) shows Wigner functions and quadrature distributions of two example states generated with $C_0 = 200$ and $C_0 = 2000$ using $M = 2$ and $M = 3$, respectively. Comparing to Fig. 2(c), we observe a clear improvement in the quality of the produced states.

The results presented in Fig. 3 are generated using the original probabilistic approach [21], as it allows efficient evaluation of the effective squeezing levels with mixed state inputs, which enables us to numerically optimize the cavity coupling rate and input squeezing levels. However, as mentioned, the protocol can be made fully deterministic following [22], with the added benefit of an expected slight increase in the squeezing levels.

Finally, we address the input squeezed light source. Ideally, one might want to use squeezed light generated from parametric down-conversion [40], as this method can yield very high-squeezing values. However, the wavelength and temporal mode profile of the squeezed light from such a source might not be straightforwardly compatible with a high cooperatively cavity QED system. In the Supplemental Material [35], we therefore propose a method to generate squeezed states starting from a coherent state, using the cavity QED system.

The results presented herein were calculated using a single-mode frequency formalism, thus assuming a negligible bandwidth of the incident optical mode. However, for fast pulsed operation, which would be desirable in order to achieve a high clock rate, the spectral width of the mode becomes relevant. Thus, for the scheme to work in this regime, the difference in the phase imposed by the cavity for the atom in state $|0\rangle$ and $|1\rangle$ should be constant across the spectrum of the pulse. In the Supplemental Material [35], we show that the phase difference is constant to second order in the pulse bandwidth if $\kappa_c = \sqrt{g^2 + 2\gamma\kappa_l + \kappa_l^2}$. If $\gamma = \kappa_l$ this approximately coincides with the value of κ_c which optimizes the balance between η and C, Eq. (10).

Conclusion.—We have presented a method for generating approximate GKP states using a cavity QED system as the central non-Gaussian element. The performance is, in practice, limited by the internal cooperativity of the systems. State-of-the-art systems have demonstrated internal cooperativities of up to 200 [30,33], which could produce approximate GKP states with 4.4 dB squeezing, which can be improved to 5.5 dB through the breeding method of Ref. [21]. However, improved cavity designs are rapidly being developed across multiple platforms, and designs with cooperativities exceeding 1000 have been proposed [41], which could push the achievable amount of effective squeezing above 10 dB in the near future.

This project was supported by the Danish National Research Foundation through the Center of Excellence for Macroscopic Quantum States (bigQ, DNRF0142).

*jhast@fysik.dtu.dk

[1] D. Gottesman, A. Kitaev, and J. Preskill, Encoding a qubit in an oscillator, Phys. Rev. A **64**, 012310 (2001).
[2] V. V. Albert, K. Noh, K. Duivenvoorden, D. J. Young, R. T. Brierley, P. Reinhold, C. Vuillot, L. Li, C. Shen, S. M. Girvin, B. M. Terhal, and L. Jiang, Performance and structure of single-mode bosonic codes, Phys. Rev. A **97**, 032346 (2018).
[3] K. Noh, V. V. Albert, and L. Jiang, Quantum capacity bounds of Gaussian thermal loss channels and achievable rates with Gottesman-Kitaev-Preskill codes, IEEE Trans. Inf. Theory **65**, 2563 (2018).
[4] N. C. Menicucci, Fault-Tolerant Measurement-Based Quantum Computing with Continuous-Variable Cluster States, Phys. Rev. Lett. **112**, 120504 (2014).
[5] I. Tzitrin, J. E. Bourassa, N. C. Menicucci, and K. K. Sabapathy, Progress towards practical qubit computation using approximate Gottesman-Kitaev-Preskill codes, Phys. Rev. A **101**, 032315 (2020).
[6] J. E. Bourassa, R. N. Alexander, M. Vasmer, A. Patil, I. Tzitrin, T. Matsuura, D. Su, B. Q. Baragiola, S. Guha, G. Dauphinais *et al.*, Blueprint for a scalable photonic fault-tolerant quantum computer, Quantum **5**, 392 (2021).
[7] M. V. Larsen, C. Chamberland, K. Noh, J. S. Neergaard-Nielsen, and U. L. Andersen, A fault-tolerant continuous-variable measurement-based quantum computation architecture, PRX Quantum **2**, 030325 (2021).
[8] W. Asavanant, Y. Shiozawa, S. Yokoyama, B. Charoensombutamon, H. Emura, R. N. Alexander, S. Takeda, J. Yoshikawa, N. C. Menicucci, H. Yonezawa *et al.*, Generation of time-domain-multiplexed two-dimensional cluster state, Science **366**, 373 (2019).
[9] M. V. Larsen, X. Guo, C. R. Breum, J. S. Neergaard-Nielsen, and U. L. Andersen, Deterministic generation of a two-dimensional cluster state, Science **366**, 369 (2019).
[10] M. V Larsen, X. Guo, C. R. Breum, J. S. Neergaard-Nielsen, and U. L. Andersen, Deterministic multi-mode gates on a scalable photonic quantum computing platform, Nat. Phys. **17**, 1018 (2021).

[11] K. Fukui, R. N. Alexander, and P. van Loock, All-optical long-distance quantum communication with Gottesman-Kitaev-Preskill qubits, Phys. Rev. Research **3**, 033118 (2021).
[12] F. Rozpędek, K. Noh, Q. Xu, S. Guha, and L. Jiang, Quantum repeaters based on concatenated bosonic and discrete-variable quantum codes, npj Quantum Inf. **7**, 102 (2021).
[13] B. W. Walshe, B. Q. Baragiola, R. N. Alexander, and N. C. Menicucci, Continuous-variable gate teleportation and bosonic-code error correction, Phys. Rev. A **102**, 062411 (2020).
[14] C. Flühmann, T. L. Nguyen, M. Marinelli, V. Negnevitsky, K. Mehta, and J. P. Home, Encoding a qubit in a trapped-ion mechanical oscillator, Nature (London) **566**, 513 (2019).
[15] B. de Neeve, T. L. Nguyen, T. Behrle, and J. Home, Error correction of a logical grid state qubit by dissipative pumping, Nat. Phys. **18**, 296 (2022).
[16] P. Campagne-Ibarcq, A. Eickbusch, S. Touzard, E. Zalys-Geller, N. E. Frattini, V. V. Sivak, P. Reinhold, S. Puri, S. Shankar, R. J. Schoelkopf *et al.*, Quantum error correction of a qubit encoded in grid states of an oscillator, Nature (London) **584**, 368 (2020).
[17] B. M. Terhal and D. Weigand, Encoding a qubit into a cavity mode in circuit QED using phase estimation, Phys. Rev. A **93**, 012315 (2016).
[18] J. Hastrup, K. Park, J. B. Brask, R. Filip, and U. L. Andersen, Measurement-free preparation of grid states, npj Quantum Inf. **7**, 17 (2021).
[19] S. Pirandola, S. Mancini, D. Vitali, and P. Tombesi, Constructing finite-dimensional codes with optical continuous variables, Europhys. Lett. **68**, 323 (2004).
[20] S. Pirandola, S. Mancini, D. Vitali, and P. Tombesi, Continuous variable encoding by ponderomotive interaction, Eur. Phys. J. D **37**, 283 (2006).
[21] H. M. Vasconcelos, L. Sanz, and S. Glancy, All-optical generation of states for "encoding a qubit in an oscillator," Opt. Lett. **35**, 3261 (2010).
[22] D. J. Weigand and B. M. Terhal, Generating grid states from Schrödinger-cat states without postselection, Phys. Rev. A **97**, 022341 (2018).
[23] D. Su, C. R. Myers, and K. K. Sabapathy, Conversion of Gaussian states to non-Gaussian states using photon-number-resolving detectors, Phys. Rev. A **100**, 052301 (2019).
[24] M. Eaton, R. Nehra, and O. Pfister, Non-Gaussian and Gottesman-Kitaev-Preskill state preparation by photon catalysis, New J. Phys. **21**, 113034 (2019).
[25] I. Tzitrin, T. Matsuura, R. N. Alexander, G. Dauphinais, J. E. Bourassa, K. K. Sabapathy, N. C. Menicucci, and I. Dhand, Fault-tolerant quantum computation with static linear optics, PRX Quantum **2**, 040353 (2021).
[26] B. Hacker, S. Welte, S. Daiss, A. Shaukat, S. Ritter, L. Li, and G. Rempe, Deterministic creation of entangled atom-light Schrödinger-cat states, Nat. Photonics **13**, 110 (2019).
[27] N. Shukla, S. Nimmrichter, and B. C. Sanders, Squeezed comb states, Phys. Rev. A **103**, 012408 (2021).
[28] K. Duivenvoorden, B. M. Terhal, and D. Weigand, Single-mode displacement sensor, Phys. Rev. A **95**, 012305 (2017).
[29] P. Lodahl, S. Mahmoodian, and S. Stobbe, Interfacing single photons and single quantum dots with photonic nanostructures, Rev. Mod. Phys. **87**, 347 (2015).
[30] D. Najer, I. Söllner, P. Sekatski, V. Dolique, M. C. Löbl, D. Riedel, R. Schott, S. Starosielec, S. R. Valentin, A. D. Wieck *et al.*, A gated quantum dot strongly coupled to an optical microcavity, Nature (London) **575**, 622 (2019).
[31] C. Y. Hu, A. Young, J. L. O'Brien, W. J. Munro, and J. G. Rarity, Giant optical Faraday rotation induced by a single-electron spin in a quantum dot: Applications to entangling remote spins via a single photon, Phys. Rev. B **78**, 085307 (2008).
[32] E. Janitz, M. K. Bhaskar, and L. Childress, Cavity quantum electrodynamics with color centers in diamond, Optica **7**, 1232 (2020).
[33] M. K. Bhaskar, R. Riedinger, B. Machielse, D. S. Levonian, C. T. Nguyen, E. N. Knall, H. Park, D. Englund, M. Lončar, D. D. Sukachev *et al.*, Experimental demonstration of memory-enhanced quantum communication, Nature (London) **580**, 60 (2020).
[34] L.-M. Duan and H. J. Kimble, Scalable Photonic Quantum Computation through Cavity-Assisted Interactions, Phys. Rev. Lett. **92**, 127902 (2004).
[35] See Supplemental Material at http://link.aps.org/supplemental/10.1103/PhysRevLett.128.170503 for analytical details of the cavity QED system, calculations of the effective squeezing levels for GKP states with a finite number of peaks, details on the optimization of the displacement amplitudes and squeezing levels, and a proposal for the generation of squeezing vacuum, which includes Ref. [36–38].
[36] C. W. Gardiner and M. J. Collett, Input and output in damped quantum systems: Quantum stochastic differential equations and the master equation, Phys. Rev. A **31**, 3761 (1985).
[37] D. F. Walls and G. J. Milburn, *Quantum Optics* (Springer Science & Business Media, New York, 2007).
[38] J. Hastrup, K. Park, R. Filip, and U. L. Andersen, Unconditional Preparation of Squeezed Vacuum from Rabi Interactions, Phys. Rev. Lett. **126**, 153602 (2021).
[39] H. Goto, S. Mizukami, Y. Tokunaga, and T. Aoki, Figure of merit for single-photon generation based on cavity quantum electrodynamics, Phys. Rev. A **99**, 053843 (2019).
[40] Henning Vahlbruch, Simon Chelkowski, Karsten Danzmann, and Roman Schnabel, Quantum engineering of squeezed states for quantum communication and metrology, New J. Phys. **9**, 371 (2007).
[41] S. Al-Sumaidae, M. H. Bitarafan, C. A. Potts, J. P. Davis, and R. G. DeCorby, Cooperativity enhancement in buckled-dome microcavities with omnidirectional claddings, Opt. Express **26**, 11201 (2018).